

QCD plasma equilibration, elliptic flow and jet-quenching – phenomena of common origin

Oliver Fochler, Andrej El, Zhe Xu and Carsten Greiner

Institut für Theoretische Physik, Goethe-Universität,
Max-von-Laue-Str. 1, D-60438 Frankfurt am Main, Germany

Abstract. Fast thermalization, a subsequent strong buildup of elliptic flow of QCD matter and jet-quenching as found at the Relativistic Heavy Ion Collider (RHIC) are understood as the consequence of perturbative QCD (pQCD) interactions within the 3+1 dimensional parton cascade BAMPS. The main contributions stem from pQCD inspired bremsstrahlung. Comparisons to Au+Au data of the flow parameter v_2 as a function of participation number as well as the gluonic contribution to the nuclear modification factor R_{AA} for most central collisions are given. Also the shear viscosity to entropy ratio is dynamically extracted, which lies in the range of 0.08 and 0.15, depending on the chosen coupling constant.

Keywords: Relativistic Heavy-ion collisions, Monte Carlo simulations, Hydrodynamic models, Particle correlations and fluctuations

PACS: 12.38.Mh, 25.75.-q, 24.10.Lx, 24.10.Nz, 25.75.Gz, 05.60.-k

The values of the elliptic flow parameter v_2 measured by the experiments at the Relativistic Heavy Ion Collider (RHIC) [1] are (nearly) as large as those obtained from calculations employing ideal hydrodynamics. This finding suggests that a fast local equilibration of quarks and gluons occurs at a very short time scale ≤ 1 fm/c. and that the locally thermalized state of matter created, the quark gluon plasma (QGP), behaves as a nearly perfect fluid exhibiting strong “explosive” collective motion. Quarks and gluons should be rather strongly coupled, pointing towards a small viscosity to entropy coefficient for the QGP. Besides the strong collective flow, jet-quenching has been observed at RHIC [2] as the second striking new discovery. So far, both phenomena could not be related by a common understanding of the underlying microscopic processes: Jet-quenching is widely thought to be described by investigating the potential energy loss on the partonic level in terms of elastic pQCD collisions and pQCD radiative processes. On the other hand, the strong elliptic flow implies early thermalization and liquid like bulk properties which can not be understood by binary pQCD collisions being considerably too weak. This has raised the speculation about nonperturbative interactions as well as about super

symmetric representations of Yang-Mills theories using the AdS/CFT conjecture.

In contrast, in this talk, it is demonstrated that perturbative QCD can still explain a fast thermalization of the initially nonthermal gluon system [3, 4, 5], the large collective effects of QGP created at RHIC [6], the smallness of the shear viscosity to entropy ratio [7, 6] and also the jet-quenching of high momentum partons [8] in a consistent manner by using a relativistic pQCD based on-shell parton cascade Boltzmann approach of multiparton scatterings (BAMPS) [3, 4].

BAMPS is a parton cascade, which solves the Boltzmann transport equation and can be applied to study, on a semi-classical level, the dynamics of gluon matter produced in heavy ion collisions at RHIC energies. The structure of BAMPS is based on the stochastic interpretation of the transition rate [3], which ensures full detailed balance for multiple scatterings. BAMPS subdivides space into small cell units where the operations for transitions are performed. Gluon interactions included in BAMPS are elastic and screened Rutherford-like pQCD $gg \rightarrow gg$ scatterings as well as pQCD inspired bremsstrahlung $gg \leftrightarrow ggg$ of Gunion-Bertsch type. The matrix elements are discussed in the literature [3, 4, 8]. The suppression of the bremsstrahlung due to the Landau-Pomeranchuk-Migdal (LPM) effect is taken into account within the Bethe-Heitler regime employing a step function in the infrared regime, allowing for independent gluon emissions.

In the present simulations, the initial gluon distributions are taken in a Glauber geometry as an ensemble of minijets with transverse momenta greater than 1.4 GeV [4], produced via semihard nucleon-nucleon collisions. The later interactions of the gluons are terminated when the local energy density drops below 1 GeV/fm³. This value is assumed to be the critical value for the occurrence of hadronization, below which parton dynamics is not valid. Because hadronization and then hadronic cascade are not yet included in BAMPS, a gluon, which ceases to interact, propagates freely and can be regarded as a free pion employing a picture of parton-hadron duality. (Implementing a Cooper-Frye prescription for hadronization and employing UrQMD for the hadronic cascade are in progress.) The minijet initial conditions and the subsequent evolution using the present prescription of BAMPS for two sets of the coupling $\alpha_s = 0.3$ and 0.6 give nice agreements to the measured transverse energy per rapidity over all rapidities [6].

As a first example the fast thermalization of gluons is demonstrated in a local and central region which is taken as an expanding cylinder with a radius of 1.5 fm and within an interval of space time rapidity $-0.2 < \eta < 0.2$. Figure 1 shows the varying transverse momentum spectrum at various early times obtained from the BAMPS calculations for central Au+Au collisions at $\sqrt{s} = 200$ AGeV. The coupling constant is taken as $\alpha_s = 0.3$. In contrast of employing only binary pQCD collisions, the spectrum reaches an exponential shape at 1 fm/c and becomes increasingly steeper at late times [3, 4]. This is a clear indication for the achievement of local thermal equilibrium and the onset of (quasi-) hydrodynamical collective expansion with subsequent cooling by longitudinal work.

As a note aside, we remark that, in addition, potential color instabilities [9] may play a role in isotropization of particle degrees of freedom at the very initial stage

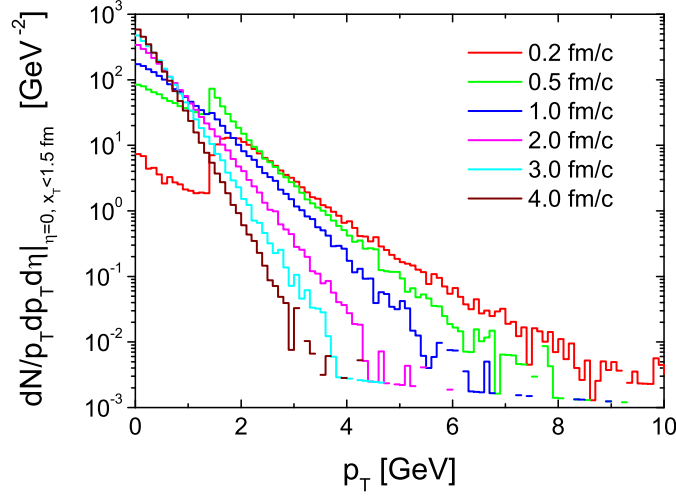


Fig. 1. (Color online) Transverse momentum spectrum in the central region at different times obtained from the BAMPS simulation of a central Au+Au collision.

where the matter is super dense. However, more quantitative studies are needed to determine their significance on the true thermal equilibration as suggested for the expanding quark gluon matter at RHIC.

The inelastic pQCD based bremsstrahlung and its back reaction are essential for the achievement of local thermal equilibrium at a short time scale. The fast thermalization happens in a similar way if color glass condensate is chosen as the initial conditions. One of the important messages obtained there is that the hard gluons thermalize at the same time as the soft ones due to the $ggg \rightarrow gg$ process, which is not included in the so called standard “Bottom Up” scenario of thermalization [5].

Kinetic equilibration relates to momentum deflection. Large momentum deflections due to large-angle scatterings will speed up kinetic equilibration enormously. Whereas the elastic pQCD scatterings favor small-angle collisions, the collision and emission angles in bremsstrahlung processes are, for lower invariant, i.e. thermal energies, rather isotropically distributed due to the incorporation of the LPM cutoff [3, 4]. Hence, although the elastic cross section is still considerably larger than the inelastic one, the given argument is the intuitive reason why the bremsstrahlung processes are acting more effectively in the equilibration of the gluon matter than the elastic interactions. Quantitatively it was shown in detail in [4] that the contributions of the different processes to momentum isotropization are quantified by the so called transport rates

$$R_i^{\text{tr}} = \frac{\int \frac{d^3 p}{(2\pi)^3} \frac{p_z^2}{E^2} C_i - \langle \frac{p_z^2}{E^2} \rangle \int \frac{d^3 p}{(2\pi)^3} C_i}{n (\frac{1}{3} - \langle \frac{p_z^2}{E^2} \rangle)},$$

where $C_i[f]$ is the corresponding collision term describing various interactions, $i = gg \rightarrow gg, gg \rightarrow ggg, ggg \rightarrow gg$, respectively. The sum of them gives exactly the inverse of the time scale of momentum isotropization, which also marks the time scale of overall thermalization. As it turns out, either by direct calculation or by the simulation, $R_{gg \rightarrow ggg}^{\text{tr}}$ is a factor of 3–5 larger than $R_{gg \rightarrow gg}^{\text{tr}}$ over a wide range in the coupling constant, which demonstrates the essential role of the bremsstrahlung for thermal equilibration [4]. For a gluon gas, which is initially far away from equilibrium, one can roughly estimate the time scale of thermalization τ_{eq} by taking the inverse of the sum of the transport collision rates close to thermal equilibrium. At temperature $T = 400$ MeV one has $\tau_{\text{eq}} \approx 1/\sum R^{\text{tr}} = 0.32$ fm/c for $\alpha_s = 0.3$. We note that the above hinges on the assumption that the system is static. Expanding systems are more complicated because particles flow, which drives the system out of local equilibrium. Therefore, the momentum degradation of flowing particles toward isotropy is slower than the inverse of the total transport collision rate [4].

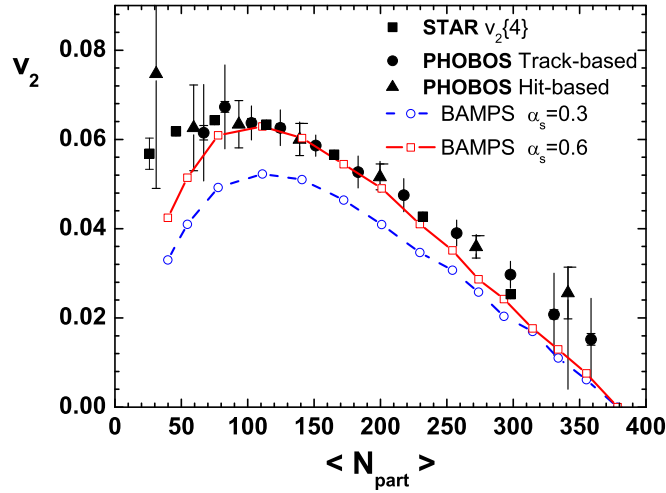


Fig. 2. (Color online) Elliptic flow $v_2(|y| < 1)$ from BAMPS using $\alpha_s = 0.3$, and 0.6, compared with the PHOBOS [10] and STAR [11] data.

Further, employing the Navier-Stokes approximation the shear viscosity η is directly related to the transport rate [7],

$$\eta \cong \frac{1}{5} n \frac{\langle E(\frac{1}{3} - \frac{p_z^2}{E^2}) \rangle}{\frac{1}{3} - \langle \frac{p_z^2}{E^2} \rangle} \frac{1}{\sum R^{\text{tr}} + \frac{3}{4} n \partial_t (\ln \lambda)},$$

where λ denotes the gluon fugacity. This expression allows to calculate the viscosity dynamically and locally in a full and microscopical simulation. On the other hand, close to thermal equilibrium the expression reduces to the more intuitive form $\eta = \frac{4}{15} \frac{\epsilon}{\sum R^{\text{tr}}}$ and thus for the shear viscosity to entropy ratio $\frac{\eta}{s} =$

$(5\beta R_{gg \rightarrow gg}^{\text{tr}} + \frac{25}{3}\beta R_{gg \rightarrow ggg}^{\text{tr}})^{-1}$. Within the present description bremsstrahlung and its back reaction lower the shear viscosity to entropy density ratio significantly by a factor of 7, compared with the ratio when only elastic collisions are considered. For $\alpha_s = 0.3$ one finds $\eta/s = 0.13$ [7, 5]. To match the lower bound of $\eta/s = 1/4\pi$ from the AdS/CFT conjecture $\alpha_s = 0.6$ has to be employed. Even for that case the cross sections are in the order of 1 mb for a temperature of 400 MeV. Perturbative QCD interactions can drive the gluon matter to a strongly coupled system with an η/s ratio as small as the lower bound from the AdS/CFT conjecture.

The elliptic flow v_2 can be directly calculated from microscopic simulations and compared to experimental data, assuming parton-hadron duality. $\alpha_s = 0.3$ and 0.6 are used for comparisons [6]. Inspecting Figure 2, except for the central centrality region the results with $\alpha_s = 0.6$ agree perfectly with the experimental data, whereas the results with $\alpha_s = 0.3$ are roughly 20% smaller. One can summarize that sufficient elliptic flow is being built up, yet the details of the freeze-out, hadronization and possible hadronic phase contributions might also give some minor dependence on the overall strength in elliptic flow, which still have to be addressed. In any case, for the QGP phase gluon bremsstrahlung dominates and yields rapid thermalization, and, therefore, early pressure buildup, and a small shear viscosity like a nearly ideal fluid.

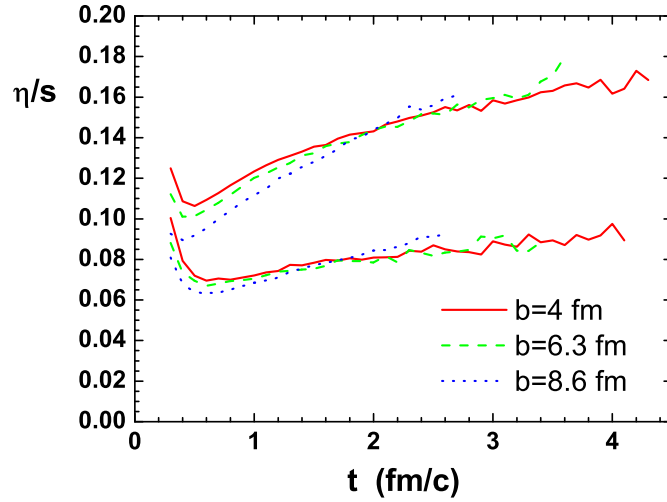


Fig. 3. (Color online) Shear viscosity to entropy density ratio η/s at the central region during the entire expansion. η/s values are extracted from the simulations at impact parameter $b = 4, 6.3$, and 8.6 fm. The upper band shows the results with $\alpha_s = 0.3$ and the lower band the results with $\alpha_s = 0.6$.

Within these simulations the ratio of the shear viscosity to the entropy density, η/s , can be locally extracted by means of the above formula. This is shown in Figure

3. As expected from the explicit expressions of the matrix elements, the ratio does not depend strongly on the gluon density or temperature, since interaction rates and transport collision rates scale with the temperature. Hence, η/s depends practically only on α_s . For $\alpha_s = 0.6$, at which the v_2 values match the experimental data, one has $\eta/s \approx 0.08$. However, η/s may be higher, since inclusion of hadronization and subsequent hadronic cascade can yield minor contributions to the final elliptic flow values. Furthermore, different picture of initial conditions (eg. color glass condensate) will also lead to different initially spatial eccentricity, and, hence, will affect the final value of v_2 and the result on η/s . These investigations are underway and will provide more constraints on extracting η/s .

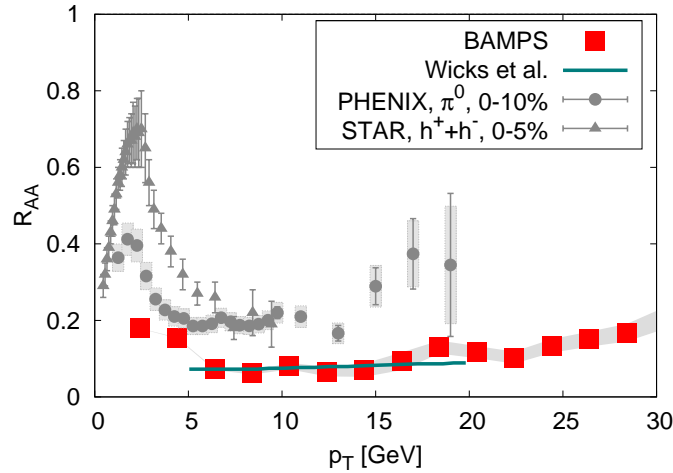


Fig. 4. (Color online) Gluonic R_{AA} at midrapidity ($y \in [-0.5, 0.5]$) as extracted from simulations for central Au+Au collisions at 200 AGeV. For direct comparison the result from Wicks et al. [14] for the gluonic contribution to R_{AA} and experimental results from PHENIX [12] for π^0 and STAR [13] for charged hadrons are shown.

The quenching of gluonic jets can now self-consistently be addressed within the same full simulation of BAMPS [8] including elastic and radiative collisions. Due to the steeply falling spectrum of initial mini-jets a suitable weighting and reconstruction scheme has to be employed, where a huge number of initial spectra are sampled which are then selected for such events for further simulation that contain high- p_T partons. The nuclear modification factor R_{AA} of the gluons is obtained directly by taking the ratio of the final p_T spectra to the initial mini-jet spectra. Fig. 4 shows the result, exhibiting a clear suppression of high- p_T gluon jets at a roughly constant level of $R_{AA}^{\text{gluons}} \approx 0.1$, potentially slightly rising towards high p_T . The coupling constant is taken as $\alpha_s = 0.3$. The dominant contribution for the energy loss are the bremsstrahlung contributions, although the picture changes for higher jet energies [8]. The suppression is approximately a factor of two stronger

than the experimental pion data. This, however, was to be expected since at present the simulation does not include quarks, which are expected to lose less energy by a factor of 4/9. Indeed, comparing with state of the art results from Wicks et al. [14] for the gluonic contribution to R_{AA} (seen as the line in Fig. 4), which in their approach together with the quark contribution reproduces the experimental data, one finds a perfect agreement.

In summary, the pQCD based parton cascade BAMPS is used to calculate the time scale of thermalization, the elliptic flow v_2 , extraction η/s , and the quenching of gluonic jets from simulations of Au+Au collisions at RHIC energy $\sqrt{s} = 200$ AGeV within one common setup. This is a committed and large scale undertaking. BAMPS includes elastic $gg \rightarrow gg$ and inelastic bremsstrahlung and its back reaction $gg \leftrightarrow ggg$. The present approach thus constitutes a first realistic 3+1 dim. microscopic transport simulation that can describe the two phenomena elliptic flow and jet-quenching by the same underlying processes. Further analyses on jet quenching, on particle correlations, on quark degrees of freedom including hadronization, on initial conditions and on the exploration and use of dissipative hydrodynamics are underway to establish a more global picture of heavy ion collisions.

Acknowledgments

We are grateful to the Center for the Scientific Computing (CSC) at Frankfurt for the computing resources. This work was supported by BMBF, DFG and GSI.

References

1. S. Adler et al. (PHENIX Collaboration), Phys. Rev. Lett. **91** 182301 (2003); J. Adams et al. (STAR Collaboration), Phys. Rev. Lett. **92** 052302 (2004).
2. C. Adler et al. (STAR), Phys. Rev. Lett. **89**, 202301 (2002); K. Adcox et al. (PHENIX), Phys. Rev. Lett. **88**, 022301 (2002).
3. Z. Xu and C. Greiner, Phys. Rev. C **71** 064901 (2005).
4. Z. Xu and C. Greiner, Phys. Rev. C **76** 024911 (2007).
5. A. El, Z. Xu, and C. Greiner, Nucl. Phys. A **806**, 287 (2008).
6. Z. Xu, C. Greiner, and H. Stöcker, arXiv:0711.0961 [nucl-th].
7. Z. Xu and C. Greiner, Phys. Rev. Lett. **100**, 172301 (2008).
8. O. Fochler, Z. Xu, and C. Greiner, arXiv:0806.1169 [hep-ph].
9. B. Schenke, M. Strickland, C. Greiner and M. H. Thoma, Phys. Rev. D **73**, 125004 (2006) A. Dumitru, Y. Nara, and M. Strickland, Phys. Rev. D **75** 025016 (2007); B. Schenke, A. Dumitru, Y. Nara, and M. Strickland, arXiv:0710.1223 [hep-ph].
10. B. Back et al. (PHOBOS Collaboration), Phys. Rev. C **72** 051901(R) (2005).
11. J. Adams et al. (STAR Collaboration), Phys. Rev. C **72** 014904 (2005).
12. A. Adare et al. (PHENIX), arXiv:0801.4020 [nucl-ex].
13. J. Adams et al. (STAR), Phys. Rev. Lett. **91**, 172302 (2003).

14. S. Wicks, W. Horowitz, M. Djordjevic and M. Gyulassy, Nucl. Phys. A **784**, 426 (2007).